DRAFT VERSION JANUARY 20, 2013
Preprint typeset using LaTeX style emulateapj v. 8/13/10

THE TEV BINARY HESS J0632+057 IN THE LOW AND HIGH X-RAY STATE

NANDA REA[1] & DIEGO F. TORRES[1,2]

Draft version January 20, 2013

ABSTRACT

We report on a 40 ks *Chandra* observation of the TeV emitting high mass X–ray binary HESS J0632+057 performed in February 2011 during a high-state of X-ray and TeV activity. We have used the ACIS-S camera in Continuos Clocking mode to search for a possible X-ray pulsar in this system. Furthermore, we compare the emission of the source during this high state, with its X-ray properties during a low state of emission, caught by a 47 ks *XMM–Newton* observation on September 2007. We did not find any periodic or quasi-periodic signal in any of the two observations. We derived an average pulsed fraction 3σ upper limit for the presence of a periodic signal of $\lesssim 35\%$ and 25% during the low and high emission state, respectively (although this limit is strongly dependent on the frequency and the energy band). Using the best X-ray spectra derived to date for HESS J0632+057, we found evidence for a significant spectral change between the low and high X-ray emission states, with the absorption value and the photon index varying between $N_{\rm H} \simeq 2.1 - 4.3 \times 10^{21}{\rm cm}^{-2}$ and $\Gamma \simeq 1.18 - 1.61$. At variance with what observed in other TeV binaries, it seems that in this source the higher the flux the softer the X-ray spectrum.

Subject headings: X-rays: binaries — stars: individual (HESS J0632+057)

1. INTRODUCTION

X-ray binary systems are one of the few astronomical objects that, under some conditions, are expected to appear as point-like TeV emitting sources when observed by instruments having the current sensitivity. That is the case of the three well-established members of the class, PSR B1259–63 (Aharonian et al. 2005a), LS I +61°303 (Albert et al. 2006), and LS 5039 (Aharonian et al. 2005b, 2006). Among these three systems, PSR B1259–63 is composed by a 48 ms pulsar in a 3.4 ys orbit with a Be companion, LS I +61°303 and LS 5039 have a ∼26 and 4 days orbital periods, and host a Be and an O start, respectively. Unfortunately the nature of the compact objects in these two binary systems is still unkown.

Of the many tens of unidentified sources discovered in the Galactic Plane H.E.S.S. survey (the survey done with the High Energy Stereoscopic System), HESS J0632+057 is one of only two unidentified very-high-energy gamma-ray sources which appear to be point-like within the experimental resolution (the other is coincident with the gravitational centre of the Milky Way; Aharonian et al. 2007).

Follow-up observations of HESS J0632+057 with *XMM–Newton* have revealed an X-ray source (XMMU J063259.3+054801) coincident with the TeV detection as well as with the massive star MWC 148 (spectral type B0pe), at a distance of ~ 1.5 kpc (Hinton et al. 2009). The chance coincidence of a massive star within the 1 arcsec error box of the brightest X-ray source in the *XMM–Newton* observation has been quantified by the latter authors to be of the order of 10^{-6}. XMMU J063259.3+054801 has in addition been found to have a hard non-thermal X-ray spectrum, and significant variability on hour timescales. These features are similar to those found in the many X-ray observations of LS I +61°303 and LS 5039 (Sidoli et al. 2006, Esposito et al. 2007; Kishishita et al. 2009; Rea et al. 2010, 2011 and references therein), strengthening the association between the TeV source and XMMU J063259.3+054801/MCW 148, and hence establishing the possibility for HESS J0632+057 to be the fourth TeV binary.

Observations conducted with the Giant Metrewave Radio Telescope (GMRT) and the Very Large Array (VLA) revealed the radio counterpart of HESS J0632+057: a point-like, low-flux, variable radio source at the position of MCW 148 was detected in both 1280 MHz with GMRT and 5 GHz with VLA (non simultaneously), with an average spectral index of –0.6 which can be generated by synchrotron-emitting electrons (Skilton et al. 2009).

Subsequent observations of HESS J0632+057 with the VERITAS array detected no significant signal from it, excluding that the source is a steady gamma-ray emitter (Acciari et al. 2009, Maier et al. 2009). Simultaneous to these TeV observations, an X-ray campaign conducted with *Swift*-XRT revealed a significant variability in the X-ray emission (Falcone et al. 2010). From this early X-ray monitoring there was no signature of an orbital periodicity for HESS J0632+057, however, assuming that the spectral variability is due to an orbital modulation, the orbital period was estimated to be larger than ~ 54 days. A similar conclusion was reached by Aragona et al. (2010) through optical spectroscopy of the massive star. Confirming the previous constraints, Bongiorno et al. (2011) recently reported an orbital period of 320±5 days, using data from the continuing long-term *Swift*-XRT monitoring campaign. By analogy with LS I +61°303 and LS 5039, the compact object hosted in HESS J0632+057 might then be a young non-accreting pulsar, or an accreting compact object (black hole or neutron star) driving a jet.

On 2011 January 23rd, *Swift*-XRT detected a rise in the X-ray flux of HESS J0632+057 (Falcone et al. 2011). The flux increase was a factor of ~ 3, which appeared similar to the rises that occurred ~ 320 and ~ 640 days before. We now know that this is the orbital period of the binary (Bongiorno et al. 2011). Motivated by this increase in X-ray activity, TeV observations were conducted by VERITAS on 2011 February 7-8, which detected the source at higher TeV flux than during the previous VERITAS campaigns (Ong et al. 2011).

[1] Institut de Ciències de l'Espai (IEEC-CSIC), Campus UAB, Torre C5, 2a planta, 08193 Barcelona, Spain
[2] Institució Catalana de Recerca i Estudis Avançats (ICREA).

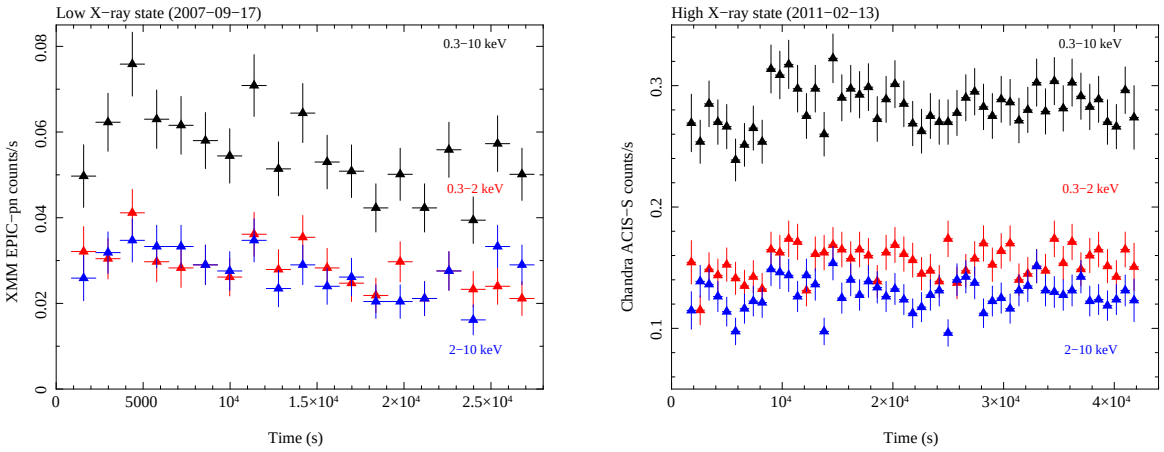

FIG. 1.— *XMM–Newton* (left panel) and *Chandra* (right panel) back-ground subtracted light-curves in the 0.3–10, 0.3–2 and 2–10 keV band, binned at 1400 s and 700 s, respectively.

These results were soon confirmed by the MAGIC collaboration (Mariotti et al. 2011). Contemporaneous with the X-ray increase, further radio observations were also conducted, which suggested the presence of slightly extended radio emission at milli-arcsec scales coincident with the position of the Be companion (Moldon et al. 2011). However, simultaneous optical observations conducted from 2011 January 5 and February 24, revealed no significant change in the radial velocities of the Be companion star (Casares et al. 2011).

During this high TeV/X-ray emission period we have conducted a 40 ks observation with the *Chandra* X-ray Observatory kindly granted to us using the Discretionary Director Time (DDT). Here we report on the spectral and timing characteristics of HESS J0632+057 during this high X-ray emission state, and we compare them with an archival *XMM–Newton* observation (Hinton et al. 2009) performed during a low X-ray emission state.

2. OBSERVATIONS AND DATA ANALYSIS

The Advanced CCD Imaging Spectrometer (ACIS) camera on board of the *Chandra* observatory (Weisskopf et al. 2000) observed HESS J0632+057, on 2011–02–13 (start time 21:15:13 (UT); Obs-ID 13237) for an exposure time of 40 ks in Continuos Clocking (CC) mode (FAINT). We have chosen this mode since it provides a time resolution of 2.85 ms, suitable for searching for fast pulsations. The CC mode also provides imaging along a single direction. The data analysis mimics that performed in Rea et al. (2010, 2011). Data were reprocessed using the CIAO software (ver. 4.3) and the *Chandra* calibration files (CALDB ver. 4.4.3). The source was positioned in the back-illuminated ACIS-S3 CCD at the nominal target position (RA 06:32:59.30; Dec +05:48:01.00; Hinton et al. 2009). Standard processing of the data was performed by the *Chandra X-ray Center* to level 1 and level 2.

We corrected the times for the variable delay due to the spacecraft dithering and telescope flexure, starting from level 1 data and assuming that all photons were originally detected at the target position. We excluded hot pixels, bad columns, and possible afterglow events. Finally, photon arrival times are in TDB and were referred to the barycenter of the Solar System using the JPL-DE405 ephemeris.

Events in the 0.3–10 keV energy range were extracted from a small region of 5×5 pixels around the source position for timing analysis, so as to reduce the background contamination in the timing analysis. The source spectrum was instead extracted from a rectangular region of 5×25 pixels around the source position, with the background being taken independently from a source-free region in the same chip.

Response matrix (RMFs) and ancillary response (ARFs) files were produced first creating a weighted image, re-binning by a factor of 8. We used this re-binned image to build the RMF file using the `mkacisrmf` tool, with an energy grid ranging from 0.3 to 10 keV in 5 eV increments. Using this RMF and the aspect histogram created with the aspect solution for this observation (`asphist`), we generated the appropriate ARF file for the source position. The source ACIS-S count rate in the 0.3–10 keV energy band was 0.265 ± 0.004 counts s^{-1} (all errors in the text are reported at 90% confidence level, unless otherwise specified).

We have also re-analized the *XMM–Newton* observation reported in Hinton et al. (2009), in search for X-ray pulsations, and with the aim of comparing the low and high X-ray state of HESS J0632+057 using the two best available spectra. The *XMM–Newton* Observatory (Jansen et al. 2001) observed HESS J0632+057 on 2007–09–17 (start time 01:22:50 (UT); obs-id 0505200101) for an exposure time of 47 ks with the EPIC-pn in Prime Full Extended Windowed mode. The addition of the two MOS cameras gave consistent results, we then decided to use only the pn camera. This observing mode results in a timing resolution of 199.2 ms, a 27.2 × 26.2 arcmin^2 field of view and only 2.3% of out of time events. Data have been processed using SAS version 11.0.0 with the most updated calibration files (CCF) available at the time the reduction was performed (April 2011). Standard data screening criteria were applied in the extraction of scientific products.

The last part of the observation was affected by proton flares which we have removed in our final products, except for the event file used for the pulsation search (which is not affected by such kind of flares), to use as much source photons as possible. Cleaning the events from the proton flare results in a good exposure time for spectral analysis of 27 ks.

We have extracted the source photons from a circular region of 15″ (such to avoid any chip gaps), centered on the source point spread function (PSF), and the background from a larger region far from the source but in the same CCD

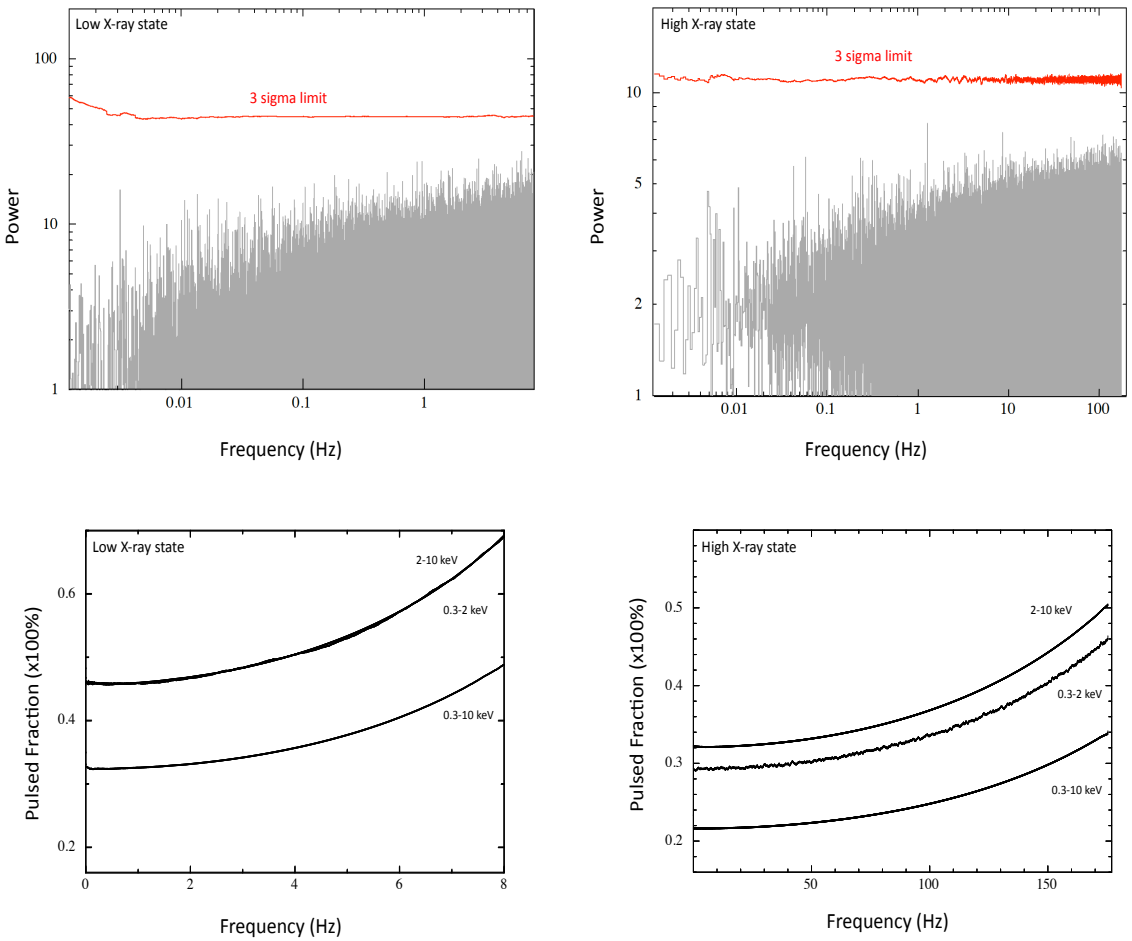

FIG. 2.— *Left column*: Timing analysis of the *XMM–Newton* data taken during a low intensity state. *Right column*: same as the left column but for the new *Chandra* data taken during a high intensity state of the source. *Top panels*: Power spectra of the two observations with the relative 3σ coherent signal detection limit. *Bottom panels*: 3σ limits on the pulsed fraction of a detectable signal in different energy bands.

(we have re-scaled the background spectrum to take into account the different extraction region with respect to the source one). For the spectral analysis we used only photons with PATTERN$\leq$4, and FLAG=0. The source EPIC-pn count rate in the 0.3–10 keV energy band was 0.064 ± 0.002 counts s^{-1}.

We report in Fig. 1 on the light-curves of the two observations we study here, which clearly show also the short-term X-ray variability of HESS J0632+057 (see also Hinton et al. 2009; Acciari et al. 2009; Falcone et al. 2010; Bongiorno et al. 2011)

3. RESULTS

3.1. *Timing analysis: search for pulsations*

We searched for periodic and quasi periodic signals in the *Chandra* and *XMM–Newton* observations performing a series of Fast Fourier Transforms (FFTs; van der Klis 1989). Given the length of our two observations ($\sim$40 ks each), the timing resolution of the *Chandra* (2.85 ms) and *XMM–Newton* (199.2 ms) observations, and the number of counts of our observations, we could search for periodic signals in the $0.005 - 175$ Hz and $0.005 - 8$ Hz frequency range, respectively[3]. Furthermore, for both data-sets we performed the search in the 0.3–10keV energy band, and also dividing the entire data set in two energy bands (0.3–2 and 2–10 keV).

For the *Chandra* data we performed an average over 7 FFTs with a bin time of 2.85 ms (see Fig. 2 right column), resulting in about 2,097,152 frequency bins for each of the 7 averaged power spectrum[4]. The resulting power-spectrum had a χ^2_ν distribution with 14 degree of freedom (dof).

For the *XMM–Newton* data we could perform a single FFT with a bin time of 60 ms (over-sampling by a factor of 3 the timing resolution of the instrument), resulting in 716,732 frequency bins in the power spectrum. The resulting power-spectrum had a χ^2_ν distribution with 2 dof (see Fig. 2 left column).

Note that given the long orbital period of HESS J0632+057 (Bongiorno et al. 2011) with respect to the exposure time of the observations we report here, we do not need to demodulate the photon arrival times for the orbital motion as we did for the 4 day TeV binary LS 5039 (Rea et al. 2011).

In calculating the 3σ detection upper limits reported in

[3] Note that in the search we have oversampled the *XMM–Newton* timing resolution by a factor of 3 to reach the 8 Hz upper bound (see Israel & Stella 1996).

[4] We could not use less FFTs because of computing limitations.

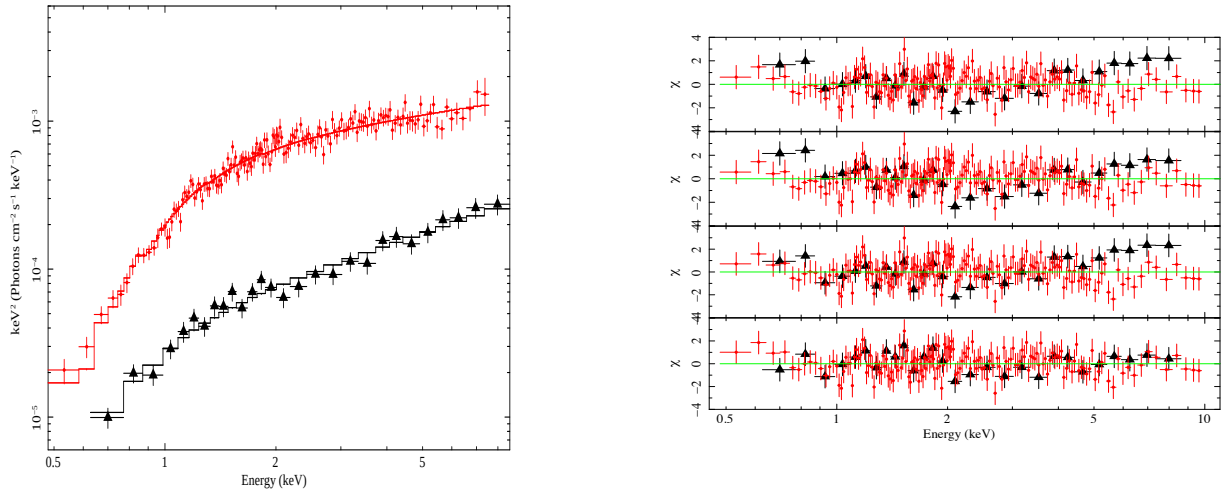

FIG. 3.— *Left panel*: Spectral energy distribution of HESS J0632+057 during the high (red; *Chandra*) and the low states (black; *XMM–Newton*) for an absorbed power-law model with all parameters free to vary among the two spectra. *Right panel*: residuals of the fits of an absorbed power-law with (from top to bottom) $N_{\rm H}$ and Γ equal for both spectra, $N_{\rm H}$ equal and Γ free, $N_{\rm H}$ free and Γ equal, and all parameters free (see text for details).

Fig. 2 we took into account for the number of bins searched, for the different dofs of the noise power distribution, and for the red-noise (Vaughan et al. 1994; Israel & Stella 1996; Rea et al. 2010). We did not find any periodic or quasi-periodic signal in any of the two observations. As a final try we attempted a joint search using both observations in a single power spectrum, with again no detection of any signal. However, note that the $\sim$3 years time-span between the two observations would likely hamper the detection of a periodic signal without the knowledge of its first derivative, and of the system precise orbital parameters.

We computed the 3σ upper limits on the amplitude of a sinusoidal signal (which we define as pulsed fraction (PF)), according to Vaughan et al. (1994) and Israel & Stella (1996). These limits range in the 0.3–10 keV energy band between PF <22–34% (0.005 – 175 Hz) and 32–48% (0.005 – 8 Hz), in the high and low X-ray state respectively (see Fig. 2 bottom panels). We also infer the same limits as a function of the energy band, which given the lower number of counts causes the energy-dependent PF limits to be slightly larger than those derived using the whole energy range in the two datasets.

3.2. *Spectral analysis*

For the spectral analysis we binned both the *Chandra* and *XMM–Newton* spectra such as to have at least 50 counts per spectral bin (see Fig.3)[5]. We first fitted both spectra together with an absorbed power-law (`phabs` and `powerlaw` models under the `XSPEC` version 12.5.0 spectral modeling program). All the absorption values we report here are referred to abundances from Anders & Grevesse (1989) and photo-electric scattering cross-section from Balucinska-Church & McCammon (1998). Fitting the two spectra with the same model with all parameters except the normalization value equal among the two spectra, results in a $\chi^2_\nu = 1.07$ (190 dof; with $N_{\rm H} = (4.0 \pm 0.2) \times 10^{21}$ cm^{-2}, $\Gamma = 1.56 \pm 0.03$). Although the χ^2_ν value is acceptable, the residuals of the *XMM–Newton* observation are clearly not satisfactory (see Fig.3). This is mirror of the fact that the large difference in counts among the two spectra make such a joint spectral fitting (and consequently the χ^2_ν value) to be dominated by the *Chandra* data.

To solve the problem of having such bad residuals, we analize possible spectral variabilities between the two spectra. In particular, we re-fit the spectra keeping the absorption value ($N_{\rm H}$) equal among the two spectra and the power-law photon index (Γ) and normalization free to vary. Although resulting in an acceptable $\chi^2_\nu = 1.07$ (189 dof; with $N_{\rm H} = (4.0 \pm 0.2) \times 10^{21}$ cm^{-2}, $\Gamma_{\rm cxo} = 1.57 \pm 0.03$ and $\Gamma_{\rm xmm} = 1.46 \pm 0.05$), the residuals of the *XMM–Newton* observation were again not good (see Fig.3). We then did a further trial keeping equal the Γ while leaving free the $N_{\rm H}$ and normalization. Again we got an acceptable $\chi^2_\nu = 1.08$ (189 dof; with $N_{\rm H,cxo} = (4.0 \pm 0.2) \times 10^{21}$ cm^{-2}, $N_{\rm H,xmm} = (3.4 \pm 0.3) \times 10^{21}$ cm^{-2}, and $\Gamma = 1.56 \pm 0.03$), but bad residuals.

Leaving all parameters free to vary for both observations we get a good $\chi^2_\nu = 0.98$ (188 dof) and better, flat-looking residuals for both *XMM–Newton* and *Chandra*. We then consider this as the best spectral modeling for both observations. In particular we find the following spectral parameters: for *Chandra* (during the high X-ray emission state), $N_{\rm H,cxo} = (4.3 \pm 0.2) \times 10^{21}$ cm^{-2}, $\Gamma_{\rm cxo} = 1.61 \pm 0.03$, and an absorbed (unabsorbed) 0.3–10keV flux of $(3.2 \pm 0.2) \times 10^{-12}$erg s^{-1}cm^{-2}($4.5 \times 10^{-13}$erg s^{-1}cm^{-2}). For *XMM–Newton* (during a low X-ray emission state): $N_{\rm H,xmm} = (2.1 \pm 0.4) \times 10^{21}$ cm^{-2}, $\Gamma_{\rm xmm} = 1.18 \pm 0.08$, and an absorbed (unabsorbed) 0.3–10keV flux of $(5.1 \pm 0.9) \times 10^{-13}$erg s^{-1}cm^{-2}($5.7 \times 10^{-13}$erg s^{-1}cm^{-2}).

To investigate further the spectral change between the two observations, we plot the statistical contours for the absorption value and the power-law photon index (see Fig.4), which clearly shows that the spectral variability among the two X-

[5] Note that the small difference in the derived spectral parameters we report in §3.2 with respect to Hinton et al. (2009), is most probably due to a different spectral re-binning used in the analysis. Anyway, all the results of our analysis of the *XMM–Newton* observation are consistent within a 99% confidence level with those reported in Hinton et al. (2009).

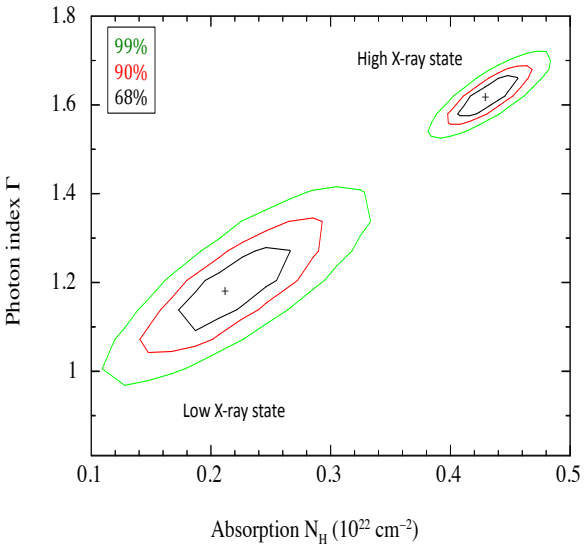

FIG. 4.— Contour plots of the absorption value ($N_{\rm H}$) and photon index (Γ) derived from the fit of the *XMM–Newton* spectrum taken while HESS J0632+057 was in a low X-ray emitting state, and of the *Chandra* spectrum during a high X-ray state. Note that the $N_{\rm H}$ refers to abundances from Anders & Grevesse (1989) and photoelectric scattering cross-section from Balucinska-Church & McCammon (1998).

ray emission state is significant at $> 99\%$ confidence level.

Assuming a distance of 1.5 kpc (Hinton et al. 2009), the system had a luminosity change between the low and the high X-ray emission state of about an order of magnitude, with $L_{\rm low} \sim 1.54 \times 10^{32}$erg s^{-1}and $L_{\rm high} \sim 1.21 \times 10^{33}$erg s^{-1}.

4. CONCLUDING REMARKS

We reported on a *Chandra* observation during the 2011 February increase of X-ray/TeV emission of the new TeV binary HESS J0632+057, which allowed us to perform the first detailed X-ray timing and spectral analysis of this source during its high state. As a comparison, we also studied the best X-ray data available in the archive for HESS J0632+057, taken while the source was in its low X-ray emission state (previously published in Hinton et al. 2009). We do not find any periodic or quasi-periodic signal from this system in any of those emission states, deriving a 3σ upper limit on the X-ray pulsed fraction of HESS J0632+057 of $\sim$30% (highly dependent on the frequency, energy range and emission state; see §3.1 and Fig.2 for details). The limits we derived for the X-ray pulsed fraction of HESS J0632+057 are similar to those derived for the archetypical TeV binaries: LS I +61°303 (Rea et al. 2010) and LS 5039 (Rea et al. 2011). Note that also the only firmly established TeV binary containing a pulsar, PSR B1259–63, does not show X-ray pulsations (Chernyakova et al. 2009). This result shows that in the pulsar scenario, the pulsar emission itself cannot be the main responsible for the X-ray emission of these TeV binaries, which is instead likely dominated by the wind-wind or intra-wind shock (unless also in this case the putative pulsar is never pointing to us during its rotation).

Also for HESS J0632+057, we find here that there exists a significant spectral variability among the low and high X-ray emission states (the flux of the new *Chandra* observation is compatible with that observed by *Swift* in the same period; Bongiorno et al. (2011)). In particular, comparing the two best available spectra, which were taken at different orbital phases, we can see $> 3\sigma$ variability in the source spectral parameters. Furthermore, while Γ increases from the low to high state by $\sim 40\%$ (hence the spectrum softens accordingly), the $N_{\rm H}$ increases by more than a factor of 2. Note also that for HESS J0632+057 we find that the higher the flux, the steeper the X-ray spectrum, which is at variance with the cases of LS 5039 and LS I +61°303, where the opposite behavior is found (Kishishita et al. 2009; Rea et al. 2010). In comparison with the other TeV binaries, we are tempt anyway to relate this spectral change with the orbital phase of HESS J0632+057. However our current ignorance on the orbital parameters of this system (beside the 320 days period; Bongiorno et al. 2011) hamper for the moment any classification of the low and high states in terms of periastron, apastron, or any of the conjunctions.

This research has made use of data from the *Chandra* X-ray Observatory and software provided by the Chandra X-ray Center. NR is supported by a Ramon y Cajal Research Fellowship to CSIC. We acknowledge the *Chandra* Director, Dr. H. D. Tananbaum, for granting us Director's Discretionary Time that allowed for this research to be done. We thank G.L. Israel for allowing the use of his DPS software and useful discussion, D. Hadasch and A. Caliandro for a quick visibility check when the source was discovered at a high flux, and the anonymous referee for useful suggestions. This work has been supported by grants AYA2009-07391 and SGR2009-811, as well as the Formosa Program TW2010005.

REFERENCES

Acciari, V. A., et al., 2009, ApJ 698, L94
Aharonian, F., et al. 2007, A&A 469, L1
Aharonian, F., et al. 2005a, A&A 442, 1
Aharonian, F., et al. 2005b, Science 309, 746
Aharonian, F., et al. 2006, A&A 460, 743
Albert, J., et al. 2006, Science 312, 177
Andres, E., Grevesse, N. 1989, Geochim. Cosmochim. Acta, 53, 197
Aragona, C., McSwain, M. V.; De Becker, M. 2010, ApJ 724, 306
Baluchinska-Church, M., McCammon, D. 1998, ApJ, 496, 1044
Bongiorno, S. D., Falcone, A. D., Stroh, M., Holder, J., Skilton, J. L., Hinton, J. A., Gehrels, N., & Grube, J., 2011, arXiv: 1104.4519, submitted to ApJ Letters
Casares, J., Ribó., M., Paredes J.M., Herrero, A., Negueruela, I., Vilardell F., 2011 Atel#3209
Chernyakova, M., Neronov, A., Aharonian, F., Uchiyama, Y., Takahashi, T. 2009, MNRAS 397, 2123
Esposito, P., Caraveo, P. A., Pellizzoni, A., de Luca, A., Gehrels, N., Marelli, M. A., 2007, A&A 474, 575
Falcone, A. D., et al 2010, ApJ 708, L52
Falcone, A., Bongiorno, S., Stroh, M., Holder, J., 2011 Atel#3152
Hinton, J., et al. 2009, ApJ 690, L101
Israel G. L., Stella L., 1996, ApJ, 468, 369
Jansen, F., et al. 2001, A&A 365, L1
Kishishita, T., Tanaka, T., Uchiyama, Y., Takahashi, T. 2009, ApJL 697, L1
Maier, G. et al. 2009, Proc. of the 31st ICRC, Lodz 2009, 0512
Mariotti, M., et al. 2011 Atel#3161
Moldon, J., Ribo, M., Paredes J.M., 2011, ATel #3180
Ong, R., et al. 2011 Atel#3153
Rea, N., Torres, D. F., van der Klis, M., Jonker, P. G., Méndez, M., Sierpowska-Bartosik, A. 2010, MNRAS, 405, 2206
Rea, N., Torres, D. F., van der Klis, M., Jonker, P. G., Méndez, M., Sierpowska-Bartosik, A. 2011, MNRAS, in press

Sidoli, L., Pellizzoni, A., Vercellone, S., Moroni, M., Mereghetti, S., Tavani, M., 2006, MNRAS 459, 901
Skilton, J. L. , et al. 2009, MNRAS 399, 317
van der Klis M., 1989, in Ogelman H., van den Heuvel E. P. J., eds, Timing Neutron Stars. Dordrecht, Kluwer, p. 27
Vaughan, B. A., et al., 1994, ApJ, 435, 362
Weisskopf, M. C., Tananbaum, H. D., Van Speybroeck, L. P., ODell, S. L., 2000, Proceedings of the SPIE, vol. 4012, pp. 216